Published by Avanti Publishers

International Journal of Architectural Engineering Technology

ISSN (online): 2409-9821

Study on the Recommended Placement and Air Distribution of Split Floor-Standing Room Air Conditioners

Zhiheng Zhang[1,3], Yibu Gao[2], Song Nie[2], Yan Tian[2], Chenxi Li[2], Ran Gao[1,2,*], Kui Yin[3], Yu Liu[3], Bo Liu[3] and Hongbin Li[3]

[1]*State Key Laboratory of Building Safety and Built Environment & National Engineering Research Center of Building Technology*

[2]*School of Building Services Science and Engineering, Xi'an University of Architecture and Technology, Xi'an, 710055, China*

[3]*China Construction Third Bureau First Engineering & MEP Co., Ltd, Shenzhen, 518110, China*

ARTICLE INFO

Article Type: Research Article

Keywords:
Place location
Air distribution
Air velocity target value
Computational fluid dynamics
Floor-standing room air conditioners

Timeline:
Received: July 06, 2022
Accepted: August 18, 2022
Published: September 14, 2022

Citation: Zhang Z, Gao Y, Nie S, Tian Y, Li C, Gao R, Yin K, Liu Y, Liu B, Li H. Study on the Recommended Placement and Air Distribution of Split Floor-Standing Room Air Conditioners. Int J Archit Eng Technol. 2022; 9: 1-17.

DOI: https://doi.org/10.15377/2409-9821.2022.09.1

ABSTRACT

In recent years, split floor-standing room air conditioners have been widely used in civil and office buildings because of their high cooling capacity and easy installation, and the air draft sensation has attracted more and more attention. In this study, a target air supply evaluation index for regional thermal comfort evaluation in the work area, the air velocity target value, is proposed. A computational fluid dynamics model for common office is established, and a total of 204 working conditions are numerically simulated for each combination of different positions, different rotation angles, and different air supply velocities (1 m/s, 2 m/s and 3 m/s) of air conditioners in the room. The influence of the rotation angle of the air conditioner on the indoor air distribution was studied, and the distribution of the indoor velocity flow field at different positions was analyzed. The air-conditioning rotation angle that makes the velocity target value of the five preset planes in the room smaller under different conditions is summarized as the recommended rotation angle. The numerical simulation results were verified by experimental means and found to be consistent with the measured results. This study can provide theoretical guidance and reference for the placement of indoor air conditioning units for users in real life.

*Corresponding Author
Email: gaoran@xauat.edu.cn
Tel: (+86) 13629284215

1. Introduction

China's building energy consumption is 947 million tons of standard coal, of which the residential sector consumes about 62%. The energy consumption of residential buildings can be divided into space cooling and heating, lighting, and household appliances, of which space cooling and heating is the most significant component of residential energy consumption [1]. The cooling consumption of split air conditioners accounts for more than 90% of the total cooling energy consumption of residential buildings [2]. Split air conditioners are the most inexpensive, easy to install, widely used, and most popular type of air conditioner [3,4]. Split vertical air conditioning systems used in office environments are superior to traditional ceiling air conditioning systems in terms of energy and thermal comfort [5]. By the end of 2020, every 100 households in China had 117.7 household air conditioners on average [6]. Typical split air conditioners can be divided into wall-mounted air conditioners and floor-standing air conditioners [7].

There are many studies on floor-standing air conditioners by domestic and foreign scholars; Huang *et al*. [8] used numerical simulation to obtain the indoor velocity field and temperature field distribution in an air-conditioned office in summer, studied and evaluated the thermal comfort and air quality of indoor personnel. Liu [9,10] evaluated the indoor air distribution of a vertical air conditioner under different deflector blade inclination angles and found that the air distribution formed by the upward inclination of the deflector blade by 4 degrees during the cooling phase had a good and rapid cooling effect; the air distribution formed by the upward inclination of the deflector blade by 33 degrees during the constant temperature phase gave the personnel the best thermal comfort. Yin *et al*. [11] used the CFD method to simulate 15 working conditions with different air supply angles of an air conditioner in an office room and determined the best air supply angle of the air conditioner itself. Zhang *et al*. [12] introduced a new smart terminal for FSACs that can be automatically adjusted by identifying the positions of humans in the room, which can effectively reduce the personnel's draft sensation and the indoor velocity target value. Li [13] studied the indoor airflow organization, personnel thermal comfort, and the satisfaction rate of the room workstations when the air conditioner was at three air supply angles: horizontal angle, upward 45° angle, and upward 60° angle. Gao [14] experimentally investigated the indoor temperature and velocity distribution of an air conditioning unit under two different deflection angles and two installation positions in a bedroom with an area of 13 m^2. Xin *et al*. [15] took a large laboratory as the research object, evaluated the efficiency of floor-standing air conditioners in different installation positions and air supply parameters, and studied the effects of different positions of vertical air conditioners on indoor air velocity, air temperature, air relative humidity, and volatile organic compounds diffusion. Summarize and sort out the above scholars' research on the air distribution of vertical air conditioners, and valuable research conclusions were given from various angles, such as the inclination angle of air conditioner guide vanes and air conditioner placement. However, few studies on "the recommended air conditioner placement and rotation angle under different air conditioner placement, different rotation angles, and different air supply velocity" are involved in the cooling of a single air-conditioner in summer. This study is a beneficial attempt at this issue.

There is a wide variety of existing indicators for the evaluation of indoor air distribution, and various studies and summaries have been conducted by different scholars, leading to valuable conclusions. Ma [16] introduced the equations for the age of air, air exchange efficiency, and ventilation efficiency, discussed the correlation between ventilation effectiveness and air distribution characteristics and derived an empirical equation for predicting replacement ventilation efficiency. Li and Zhao [17] compiled and explained in detail common indoor air distribution evaluation indexes, such as the age of air, air exchange efficiency, velocity uniformity coefficient, temperature uniformity coefficient, discharge efficiency, and accessibility of pollution sources, which provided great reference value for the research evaluation of air distribution. Fanger [18] first proposed the predicted mean vote and predicted percent dissatisfaction (PMV-PPD) indicators for predicting the average vote and the percentage of dissatisfaction, which filled the gap in thermal comfort evaluation indicators. Wang *et al*. [19] revised air diffusion performance indices (ADPIs) which were developed for bedrooms for cooling and heating modes and used revised ADPIs to identify an optimum positioning for the installation of reversible room air-conditioners in the bedroom for maximum thermal comfort. Liu [9,10] improved two evaluation indexes, air diffusion performance index (ADPI) and energy utilization coefficient (EUC), and proposed a new evaluation index, the fast cooling effect index (FCEI), which can effectively evaluate the fast cooling effect of air diffusion. Two issues need to

be paid attention to in evaluating the air supply of split floor-standing air conditioning in this study. One is air accessibility; that is, air should be supplied to the working area (target air supply area) where humans are located. The other is the draft sensation; that is, the draft sensation should be reduced at the position of the air supply. How to describe the above two problems with an evaluation index is the problem that this study tries to solve.

This paper proposes a target air supply evaluation index for evaluating air supply effect in the working area, adopts a research method combining numerical simulation and full-size experiment, establishes a computational model, studies the recommended rotation angle of floor-standing air conditioner in different indoor locations and different air supply velocity analyzes the indoor velocity flow field distribution at different locations. This study will provide theoretical guidance for users' indoor air conditioner placement in real life.

2. Idea Generation

2.1. Velocity Target Value

The previous series of studies [20,21] defined the air velocity target value as shown in equation (1), which comprehensively reflects the deviation of the actual air velocity within and outside the occupied zone from the expected air velocity:

$$T_{\mathrm{r}}=\sqrt{\frac{\sum_{1}^{n_1}(\mathrm{v}_1-\mathrm{v}_1^{'})^2+\sum_{1}^{n_0}(\mathrm{v}_0-\mathrm{v}_0^{'})^2}{(\mathrm{n}_1+\mathrm{n}_0)}} \tag{1}$$

Where: T_r refers to the velocity target value; n_1 is the number of measurement points within the occupied zone; n_0 is the number of all measurement points outside the occupied zone; v_1 and v_1' are the actual air velocity and the expected air velocity of the measuring points in the occupied zone respectively, m/s; v_0 is the actual air velocity of measurement points outside the occupied zone, m/s; v_0' is the expected air velocity of the measurement points outside the occupied zone (since no wind is expected in this area, so v_0' = 0 m/s).

In order to effectively target air supply and save energy, equation (1) considers the velocity field in the entire room, i.e., the velocity field in the working area shall be considered to make it as close as possible to the expected air velocity, and meanwhile try to avoid air supply outside the working area. In this study, we only need to consider the velocity field in the occupied zone (air supply target area) under the air conditioner and consider how to reduce draft sensation in the occupied zone of the personnel, the velocity field outside the occupied zone is not considered, so the velocity target value is defined as：

$$T_{\mathrm{v}}=\sqrt{\frac{\sum_{\mathrm{i}=0}^{\mathrm{n}}(\mathrm{v}_{\mathrm{i}}-\mathrm{v}_{\mathrm{t}})^2}{\mathrm{n}}} \tag{2}$$

Where, T_v refers to the velocity target value; n refers to the number of measurement points in the occupied zone; v_i is the air velocity of point i within the occupied zone (obtained by numerical simulation or experimental method), v_t is the expected air velocity in the occupied zone, specified as 0.3 m/s in this study. The closer the velocity v_i is to the expected air velocity v_t, the better the air supply effect is.

2.2. Air-Conditioning Room Model and the Occupied Zone

The physical model in this paper is selected for a conference room with length, width, and height of 7.7 m, 5.6 m, and 3.0 m, respectively. The vertical air conditioner consists of indoor and outdoor units. The outdoor unit mainly consists of a condenser, compressor, and fan, while the indoor unit contains a fan, evaporator, air outlet, and air inlet, and these two units are connected with copper pipes. The length, width, and height of the indoor air conditioner unit in this study are 0.50 m, 0.33 m, and 1.78 m, respectively. The size of the air outlet is 0.45 m × 0.28 m, and the size of the air inlets on both sides is 0.07 m × 0.8 m. Fig. **1** shows a schematic diagram of several planes and the occupied zone divided when the air conditioner is placed in the X direction (the short side of the room) and the Z direction (the long side of the room).

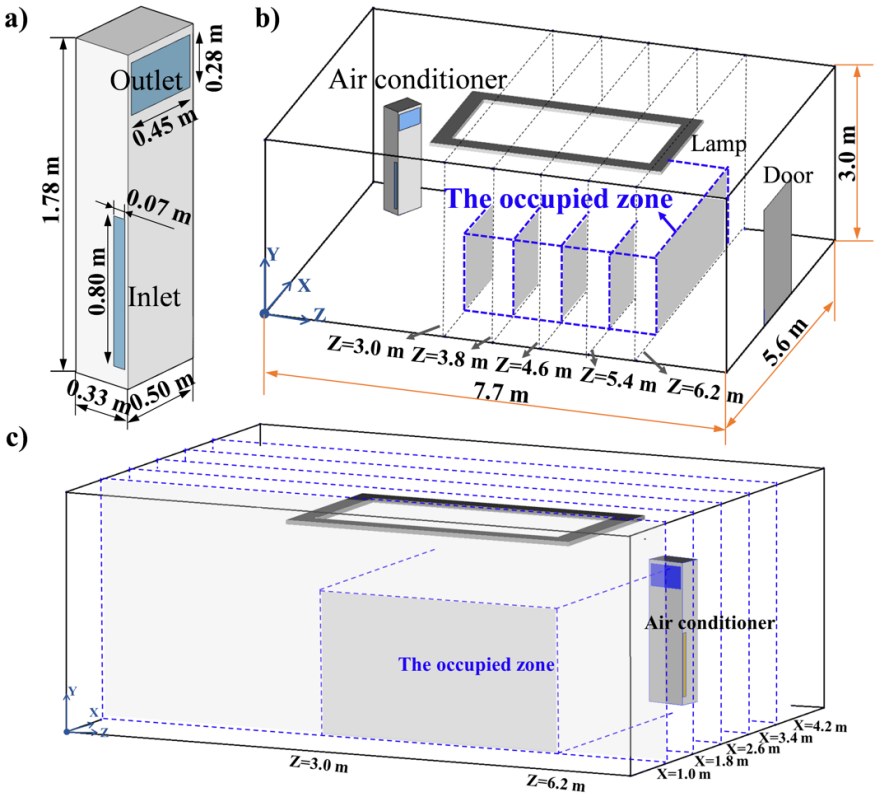

Figure 1: (a) Dimensions of the air conditioner; (b) several planes and the occupied zone when the air conditioner is placed in the X direction (short side of the room); (c) several planes when the air conditioner is placed in the Z direction (long side of the room).

2.3. Schematic Diagram of Different Air Conditioning Positions

As shown in the top view of the room in Fig. **2**, it is assumed that there are four different air conditioner locations numbered "①, ②, ③, ④" in the X direction (the short side of the room) with the same distance of 0.8 m.

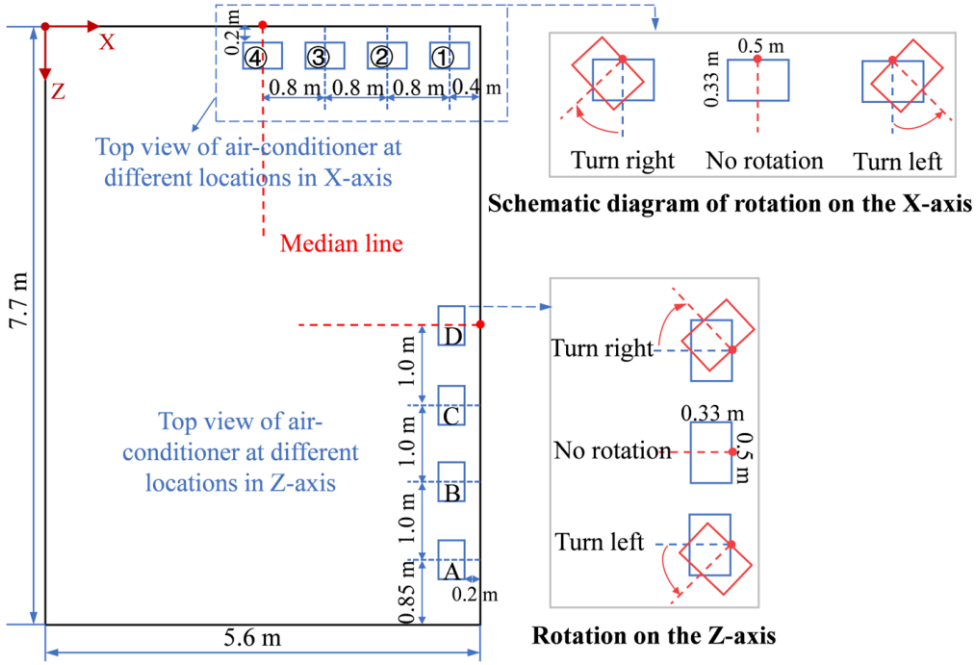

Figure 2: Top view of different air conditioner locations and rotation angle.

Location ④ is on the center median of the short side of the room, and no other locations will be extended due to the symmetry of the room. It is assumed that there are four different locations numbered "A, B, C, D" in the Z direction (the long side of the room), with the same distance of 1.0 m, and position D is on the median line of the long side. When the rear wall of the air conditioner is placed parallel to the wall, the rear wall of the air conditioner is 20 cm away from the room wall. Then rotate the air conditioners in different locations at different angles, and determine the direction of the left or right turn from the perspective of the air conditioner itself. The base point of rotation is the center point of the intersection between the rear wall of the air conditioner and the ground. It is assumed that there are many situations such as no rotation, left rotation of 10°, 20°, 30°, 40°, right rotation of 10°, 20°, 30°, 40°. Therefore, there are several rotation cases at each position, and the combined working conditions are shown in Table **1**. Combined with the air conditioning outlet velocity settings of 1 m/s, 2 m/s, and 3 m/s, a total of 204 working conditions are simulated.

Table 1: All working conditions at different air conditioning locations combined with different rotation angles.

Rotation Situation / Different Locations	No Rotation	Turn Left	Turn Right	Working Conditions
Location ① and Location A	0°	10°/20°	10°/20°/30°/40°/50°	16
Location ② and Location B	0°	10°/20°	10°/20°/30°/40°/50°	16
Location ③ and Location C	0°	10°/20°/30°/40°	10°/20°/30°/40°	18
Location ④ and Location D	0°	10°/20°/30°/40°	10°/20°/30°/40°	18

3. Research Methods

This paper adopts the method of combining full-scale experiments with CFD numerical simulation. The experimental method can accurately measure the velocity value of indoor measuring points and can also be used to test the accuracy of numerical simulation settings to modify its parameter settings. The numerical simulation method is particularly suitable for various working conditions in this study, which can save manpower to a large extent and visually see the indoor flow field, which is conducive to the analysis of the distribution of air distribution in the vertical air conditioning room.

3.1. CFD Numerical Simulation

3.1.1. Turbulence Model

The airflow is treated as a continuum by the Reynolds-averaging method for calculating turbulent effects. In steady state conditions, the continuity equation can be written as:

$$\frac{\partial \rho}{\partial \tau} + \frac{\partial}{\partial x_i}\left(\rho u_i\right) = 0 \tag{3}$$

Momentum equation:

$$\frac{\partial}{\partial \tau}\left(\rho u_i\right) + \frac{\partial}{\partial x_j}\left(\rho u_i u_j\right) = -\frac{\partial p}{\partial x_i} + \frac{\partial}{\partial x_j}\left(\eta \frac{\partial u_i}{\partial x_j} - \rho\overline{u_i' u_j'}\right) + S_i \tag{4}$$

In the momentum equations, $(\rho\overline{u_i' u_j'})$ are the Reynolds stresses. Introducing the Boussinesq assumption, the items can be given as:

$$-\rho\overline{u_i'u_j'} = -p_t\delta_{i,j} + \eta_t\left(\frac{\partial u_i}{\partial x_j} + \frac{\partial u_j}{\partial x_i}\right) - \frac{2}{3}\eta_t\delta_{i,j} \tag{5}$$

Energy equation:

$$\frac{\partial}{\partial\tau}(\rho T) + \frac{\partial}{\partial x_j}(\rho u_j T) = \frac{\partial}{\partial x_j}\left(\Gamma\frac{\partial T}{\partial x_j} - \rho\overline{u_j'T'}\right) + S \tag{6}$$

In the energy equations, item $-\rho\overline{u_i'T'}$ can be expressed as:

$$-\rho\overline{u_i'T'} = \Gamma_t\frac{\partial T}{\partial x_j} \tag{7}$$

Where ρ is the density of air, kg/m^3; τ is time, s; x_i, x_j is distances along coordinate axes, m; u_i, u_j is the mean velocities along coordinate axes; η is molecular viscosity of air, m^2/s; η_t is turbulent viscosity, m^2/s; $\delta_{i,j}$ is Kronecker delta; u_i', u_j' is fluctuating velocities along coordinate axes, m/s; T is mean temperature, K; Γ is molecular diffusivity, kg/m/s; Γ_t is turbulent diffusivity, kg/m/s; S is source item in the energy equation.

The turbulence model is closely related to the accuracy and economy of the simulation results. The Realizable k-ε model can better simulate the air supply jet problem [22].This turbulence model is also used in previous research on the air distribution of vertical air conditioning [9]. Therefore, this study first attempts to use the Realizable k-ε model. At the same time, the simulated and measured velocity values of measuring points in the Z=3.0 m plane when the air conditioner turns right at location ① to 20° are compared. The results show that the simulated results of the Realizable k-ε turbulence model are closest to the measured value compared with other common models (Standard k-ε, RNG k-ε, SST k-ω and Standard k-ω), which further verifies the reliability of using Realizable k-ε model to simulate indoor velocity field in this study.

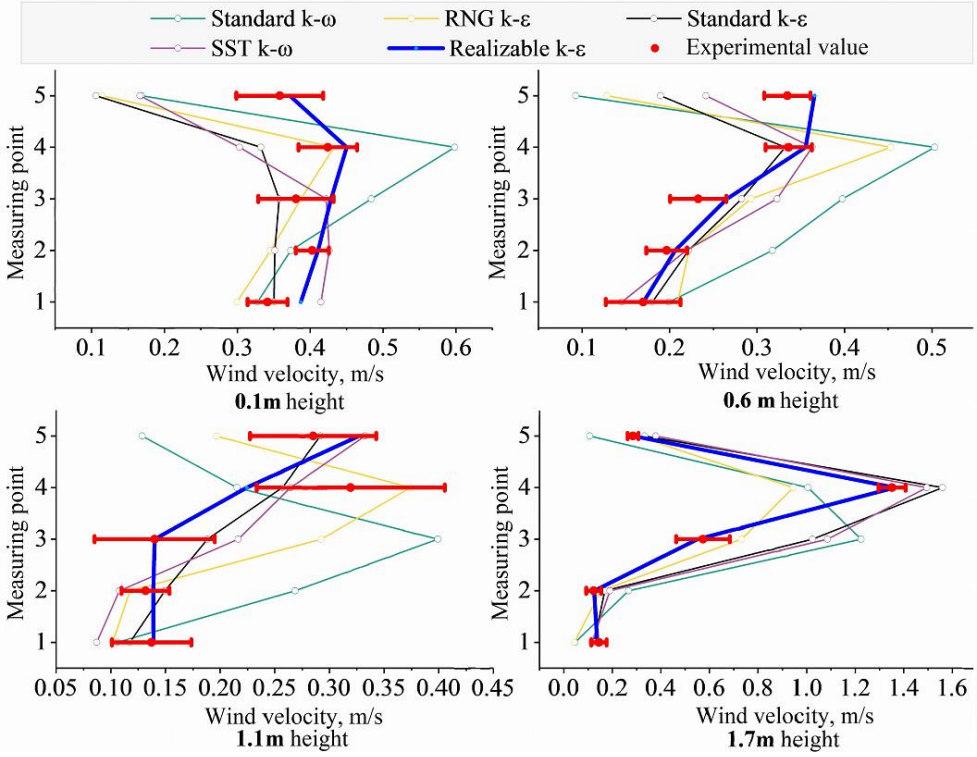

Figure 3: Turbulence model verification.

3.1.2. Setup of the Solvers

Turn on the gravity acceleration and select the energy equation solver. In order to consider the influence of air density change caused by the temperature difference on airflow movement, the Boussinesq hypothesis is introduced to help deal with the buoyancy term [23]. The simulation adopts a steady-state and pressure-based solver, and the discrete scheme is set to a second-order upwind scheme. The SIMPLE algorithm is used to couple pressure and velocity [24]. Assuming that the indoor air is a steady flow, it is not affected by the external airflow. It is considered that indoor air tightness is good, and the influence of short-term opening and closing doors on indoor airflow is ignored.

In this study, the air supply is considered as the normal direction of the outlet, and the outlet adopts the velocity-inlet boundary condition. The outlet velocity is set to 1 m/s, 2 m/s, and 3 m/s, respectively, the air supply temperature is set to 298 K, and the turbulence intensity is set to 5 %. The outflow boundary condition was adopted at the return air outlet. The room wall is set as the constant wall temperature 293k condition with roughness k=0.025mm, no velocity slip, and no velocity permeability.

3.1.3. Grid Partition and Independence Verification

A good grid is a key to successful calculation and accurate solutions. In order to simulate the indoor flow field more accurately, the flow field in the area where the velocity gradient changes greatly needs to be densified, so it is necessary to ensure that the grid division at the outlet and the return outlet is more detailed. The room adopts the hybrid grid structure, and the grid quality is above 0.3. The element quantities of 1442K, 2729K, 3419K, and 4356K are solved, respectively. It is found that when the number of grids is 3419K, continuing to encrypt the grid will not have a great impact on the velocity distribution, so the element quantity is taken as 3419K.

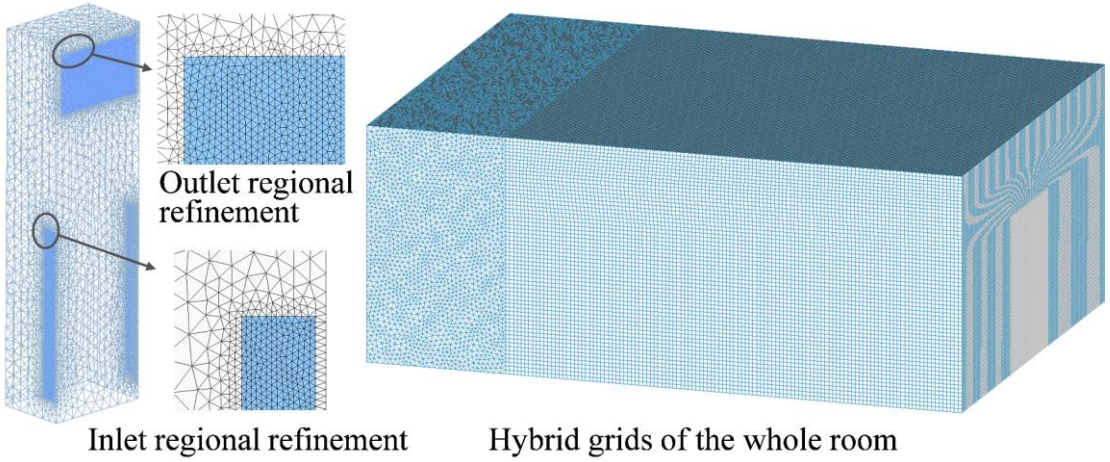

Figure 4: Grid division diagram.

3.2. Full-Scale Experiment

3.2.1. Experimental Instrument

The parameter to be measured in this study is air velocity, so Swema 03 anemoscope is used. The measuring range of Swema 03 is 0.05~3 m/s, the measuring resolution is 0.01 m/s, the measuring accuracy is ±3 %, and the response time is T_{90} < 0.2 s. During the test, the time constant of the anemoscope was set to 0.1 s and the recording interval to 0.25 s.

According to ASHRAE 55 [25] requirements, measurements were carried out at four heights of 0.1 m, 0.6 m, 1.1 m, and 1.7 m. According to the range of air supply targeted area, 20 representative measuring points were evenly divided and selected, as shown in Fig. **5**.

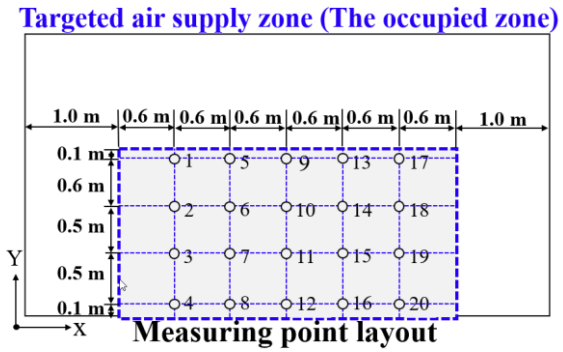

Figure 5: The layout of measuring points when air conditioning is placed on the short side.

3.2.2. Measurement Process and Experimental Error

Before measuring, locate each measuring point with a ruler, and mark it with a striking red on the ground. During the measurement, the Swema 03 anemometer is fixed on the tripod (small tripods are used at the height of 0.1 m and 0.6 m, and large tripods are used at the height of 1.1 m and 1.7 m), as shown in Fig. **6**. The level gauge and the measuring calibration board are used for calibration every time the measurement point is changed.

In the measurement process, to ensure that the uniformity of air-conditioning outlet is consistent with the numerical simulation, the air-conditioning transverse flap was in a horizontal state, i.e., no deflection occurs, so the airflow level does not deflect into the room.

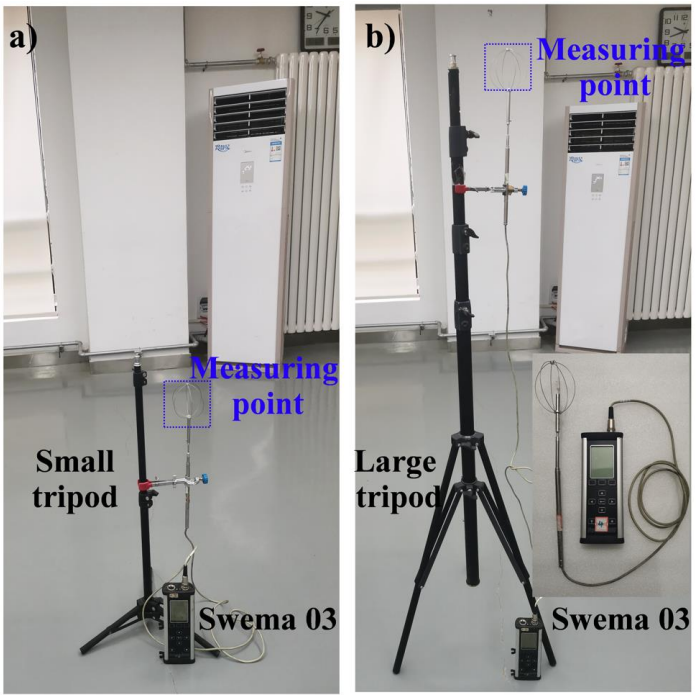

Figure 6: (a) The test diagram when the instrument is fixed with a small tripod at the height of 0.6 m; (b) the test diagram when the instrument is fixed with a large tripod at the height of 1.7 m.

During the actual operation of the air conditioner, its outlet air velocity fluctuates to some extent. To ensure that the air velocity of the measurement point is measured under the condition that the outlet air velocity of the air conditioner is 3 m/s, one Swema 03 anemoscope is placed in front of the air conditioner outlet and one at the measurement point, and the two devices start and stop simultaneously. The outlet air velocity of the air conditioner beyond the range of 3 ± 0.05 m/s and the recorded data of the measurement point at the same time are excluded. In this way, we can ensure the reliability of the measurement data after the useless data are eliminated.

The measurement time at each point is 4 minutes. After the measurement starts, the tester should quickly move away from the measurement area and return and turn off the instrument after four minutes. Since the movement of the tester within 10s after the beginning of the test and 10s before the end of the test may affect the accuracy of the results, the data in this period should also be eliminated, which can effectively ensure the accuracy of the data.

The errors in this experiment are mainly random errors, which are caused by the experimental operation process. The standard deviation is used to calculate the error of the air velocity of the 20 measuring points:

$$\sigma = \sqrt{\frac{1}{N}\sum_{i=1}^{N}(x_i - \overline{x})^2} \tag{8}$$

Where σ is the standard error; N is the number of measurement points, N=20; x_i is the velocity value at the measurement point in units of m/s; $\overline{x}$ is the average air velocity value at the measuring point, m/s, take $\overline{x}$ as the actual velocity value of the measuring point, Fig. **7** shows the standard error of the measurement point.

The difference between Tv and standard deviation σ are as follows: (1) The formula format is different; (2) the velocity value in formula σ is measured by 20 measuring points, and the velocity value in T_V is obtained from the data of thousands of nodes in the numerical simulation.

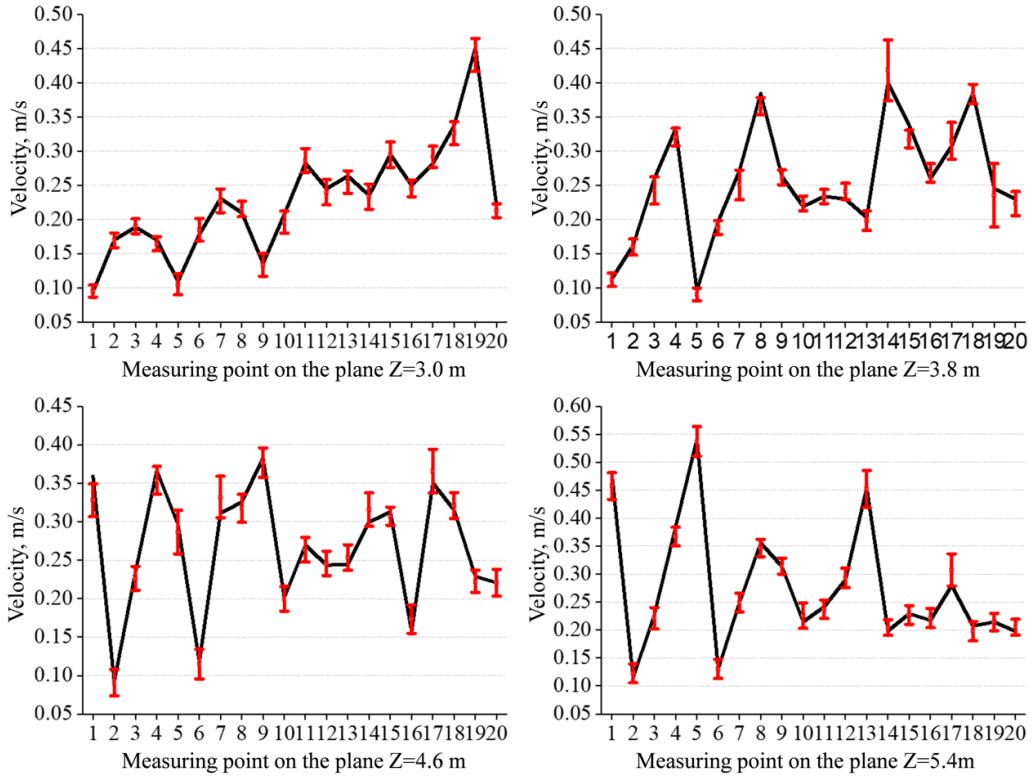

Figure 7: Comparison of experimental and simulated values at different planes.

4. Research Results

4.1. Experimental Verification

The velocity field at the measurement points in the work area was measured experimentally when the air conditioner was fed with a 20° right turn at position ① to ensure the reliability of the study. As shown in Fig. **7**, the simulated derived value and the experimentally measured value fit well at the measurement points in each plane within the flow field, indicating that the simulation results can better reflect the actual flow field in the office where

floor-standing air conditioners are installed, which illustrates the reasonableness and applicability of the simulation model.

A few measurements have errors, and the reasons for the small errors between the experimental results and the simulated value may be: (1) the physical model of the office is simplified and does not take into account the influence of obstacles such as air leakage from doors and windows, tables and chairs on the indoor velocity field; (2) There are some errors in the numerical model, such as rounding errors and discretization errors; (3) There are small differences between the boundary conditions set in the calculation and the actual conditions, for example, the walls are set as constant wall temperature boundary conditions in the simulation, while in the actual situation, the indoor wall temperature will fluctuate slightly with time and will not remain constant due to the influence of radiation and convection heat transfer conditions.

4.2. Recommended Rotation Angles for Each Position at Different Air Supply Velocity

In this section, the recommended rotation angles for different locations in the X and Z directions of the room are discussed for the cases of 1 m/s, 2 m/s, and 3 m/s air outlet velocities of the air conditioner, respectively. After the numerical simulation is completed, the velocity target value is derived for each node velocity calculation in different plane working areas.

At different locations in the Z direction of the room, the velocity target value and its average value in the working area of the five planes X=1.0 m, X=1.8 m, X=2.6 m, X=3.4 m, X=4.2 m are taken as the evaluation reference. At different locations in the X direction, the velocity target value and its average value in the working area of Z=3.0 m, Z=3.8 m, Z=4.6 m, Z=5.4 m, and Z=6.2 m are taken as the evaluation reference. The angle that makes "the lowest velocity target value of five planes and the lowest average value" the most is determined as the recommended rotation angle. In Fig. **8** to Fig. **13**, the dotted line represents left rotation, the solid line represents right rotation or no rotation, and different colors represent different rotation angles.

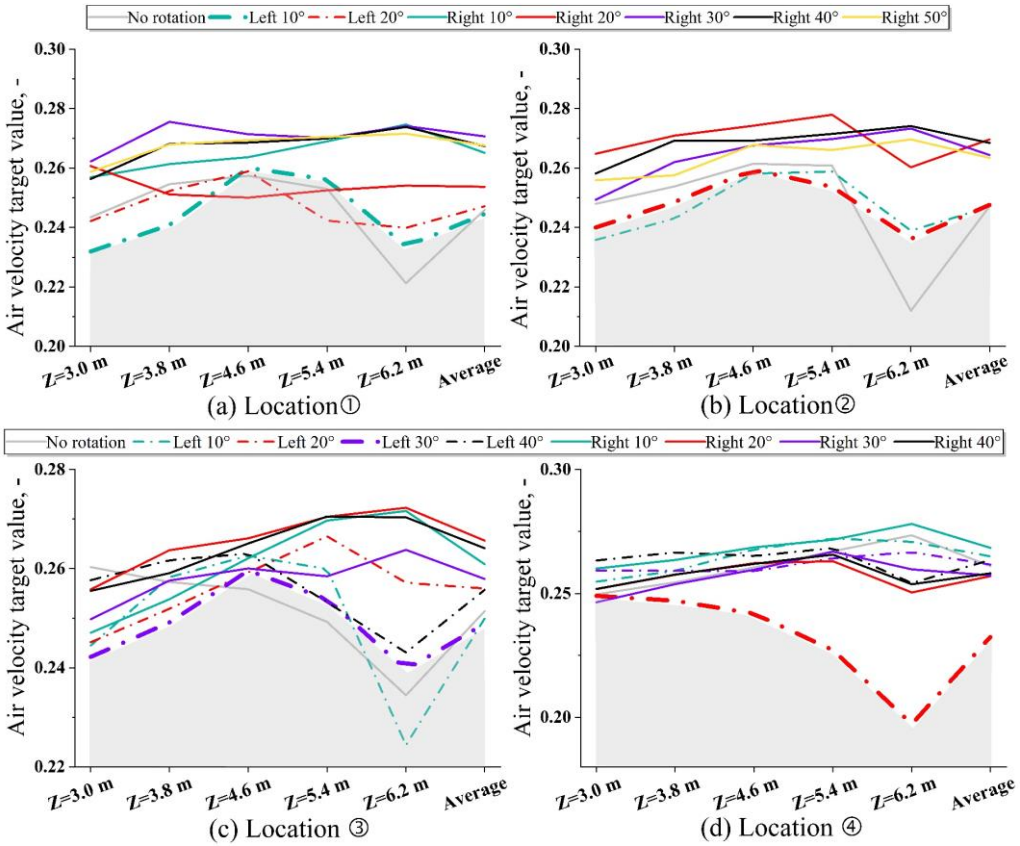

Figure 8: Recommended rotation angles for different locations in the X direction (short side of the room) when the air supply velocity is 1 m/s.

4.2.1. Recommended Angle when Air Supply Velocity is 1 m/s

From the comparison in Fig. **8**, it can be obtained that at position ①, when the air conditioner is turned left by 10°, the velocity target value in two planes is the smallest, and the average value of five planes is also the smallest. At position ②, when the air conditioner is turned left by 20°, the overall situation is better. At position ③, when the air conditioner is turned left by 30°, the target value of two planes and the average value of five faces is the smallest; at position ④, when the air conditioner is turned left by 20°, the target value of five planes and its average value are the smallest. The above angle can be regarded as the recommended rotation angle of the air conditioner with the best air supply effect.

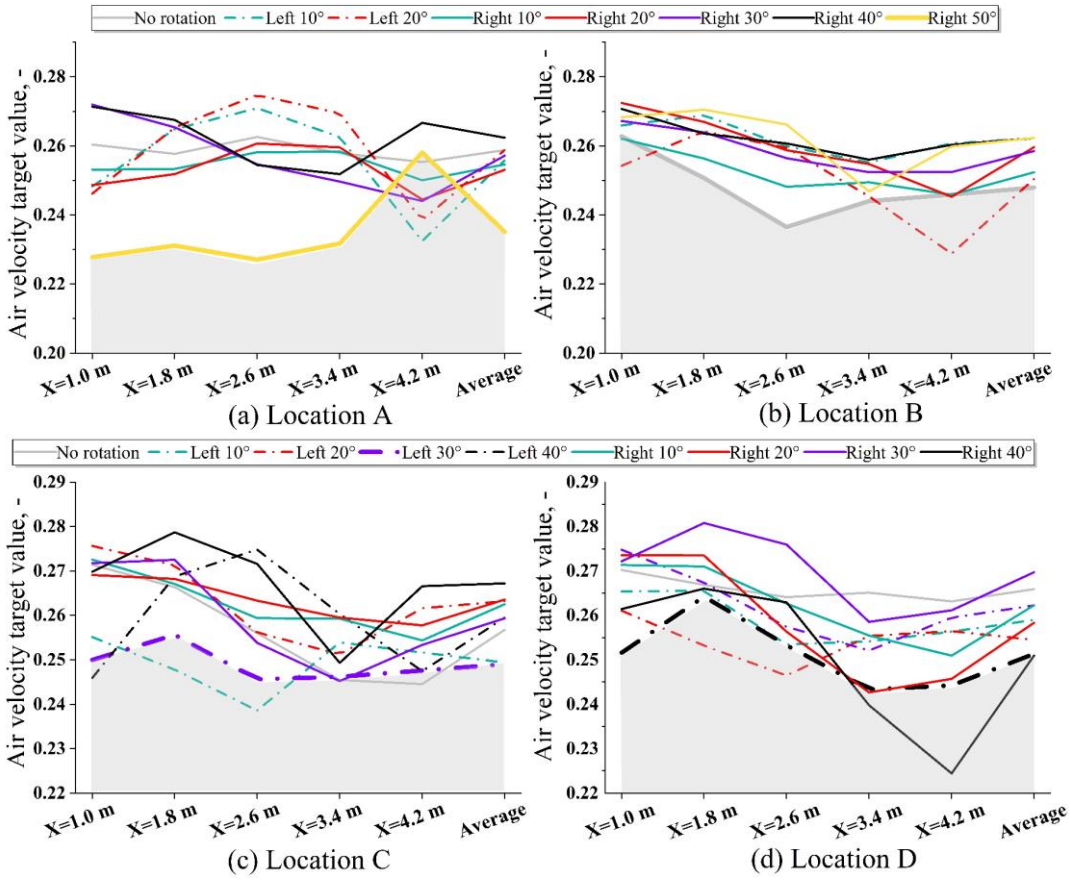

Figure 9: Recommended rotation angles for different positions in the Z-direction (long side of the room) when the air supply velocity is 1 m/s.

From the comparison in Fig. **9**, it can be seen that at position A, when the air conditioner is rotated to the right at 50°, except for the X=4.2 m plane, all other values are at the minimum. At position B, when the air conditioner is not rotated, three planes and the average value are at the minimum. At position C, when the air conditioner is rotated to the left at 30°, the overall velocity target value is distributed more evenly. At position D, when the air conditioner is rotated to the left at 40°, two and five planes are at the minimum. The above angle can be regarded as the recommended rotation angle of the air conditioner.

From Fig. **8** and Fig. **9**, we can find that at locations ①, ②, ③, and ④, most of the velocity target values fall in the range of 0.22-0.28; at locations A, B, C, and D, most of the velocity target value fall in the range of 0.24-0.28, which is not much different from each other. Therefore, when the air conditioning outlet velocity is 1 m/s, the rotation angles analyzed above to make the best air supply effect are only a relatively better value, and other rotation angles are also available to meet the requirements. For example, at position ②, the overall velocity target value of the air conditioner turned 10° left is also small; at position C, the average value of its five planes' velocity target values is also the smallest. When the air conditioner turns 10° to the left, which can also be regarded as a better parameter value.

4.2.2. Recommended Angle when Air Supply Velocity is 2 m/s

From the comparison in Fig. **10**, we can see that at position ①, when the air conditioner is turned right by 50°, there are two planes and five planes average with the smallest average value; at position ②, when the air conditioner is turned left by 20°, the air supply effect is the best; at position ③, when the air conditioner is turned left by 20°, the overall effect is better and the air supply effect is considered the best; at position ④, when the air conditioner is turned right by 30°, the target value of two planes and the average value of five planes is the smallest, and the above angle is the recommended rotation angle.

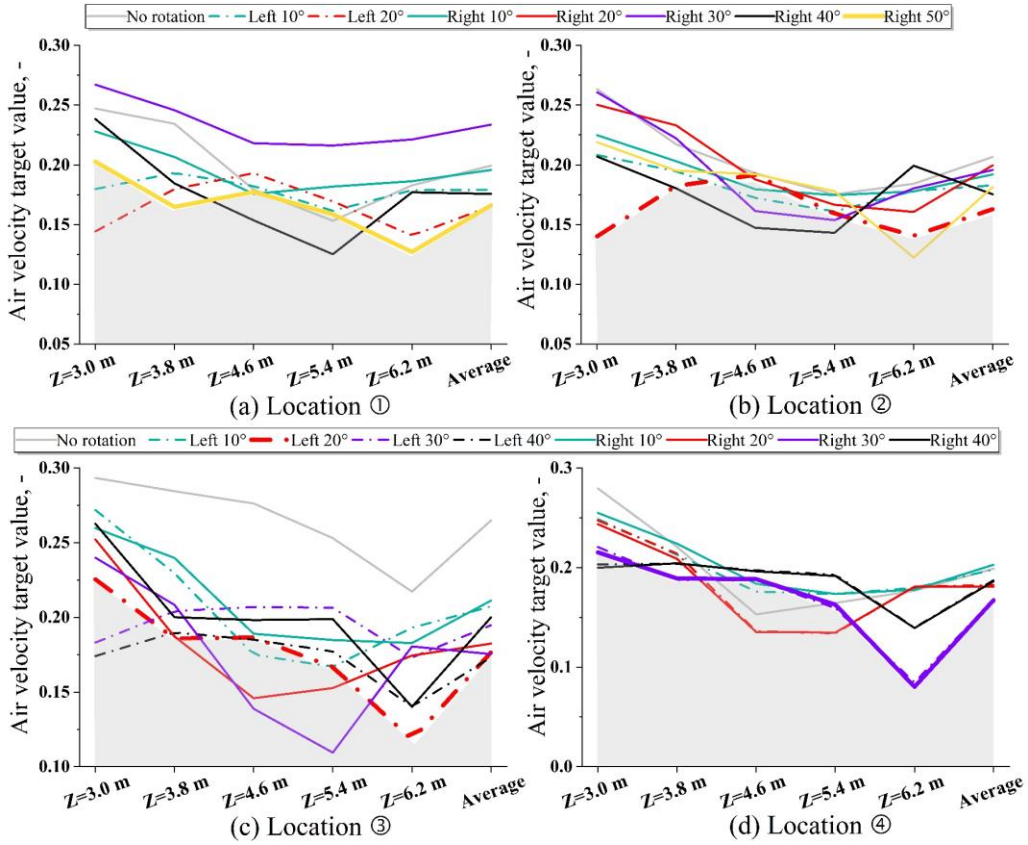

Figure 10: Recommended rotation angles at different locations in the X direction (short side of the room) at 2 m/s.

From the comparison in Fig. **11**, it can be seen that at position A, the velocity target value and their average value within the working area of the five planes are the smallest when the air conditioner is rotated left at 20; at position B, when the air conditioner is rotated left at 20°, the X=1.0 m, X=1.8 m and X=2.6 m plane targeting value are on the smaller side, and the others are at the minimum; at position C, when the air conditioner is rotated left at 40°, the overall velocity targeting value is smaller; at position D, the air conditioner turns right at 40°, except for two planes with the slightly larger target value, all other values are at the minimum, and the above angles are set as the recommended rotation angles for the four locations.

From Fig. **10** and Fig. **11**, it can be seen that the fluctuation range of the velocity target value of the five planes is larger than that of 1 m/s, with most of the values concentrated in the range of 0.1-0.3. The reason is that as the air velocity increases, the farther the indoor location from the air outlet, the more the velocity decays and the greater the change, so the greater the change in the velocity target value.

4.2.3. Recommended Angle when Air Supply Velocity is 3 m/s

From the comparison in Fig. **12**, it can be seen that at position ①, when the air conditioner is rotated 10° left, the velocity target value of three planes and the average value of five planes are the smallest; at position ②, when the air conditioner is rotated 20° left, the velocity target value of three planes and the average value of five planes are the smallest; at position ③, when the air conditioner is rotated 40° left, the air supply effect is the best; at

position ④, when the air conditioner is not rotated, the overall velocity target value is smaller and more evenly distributed.

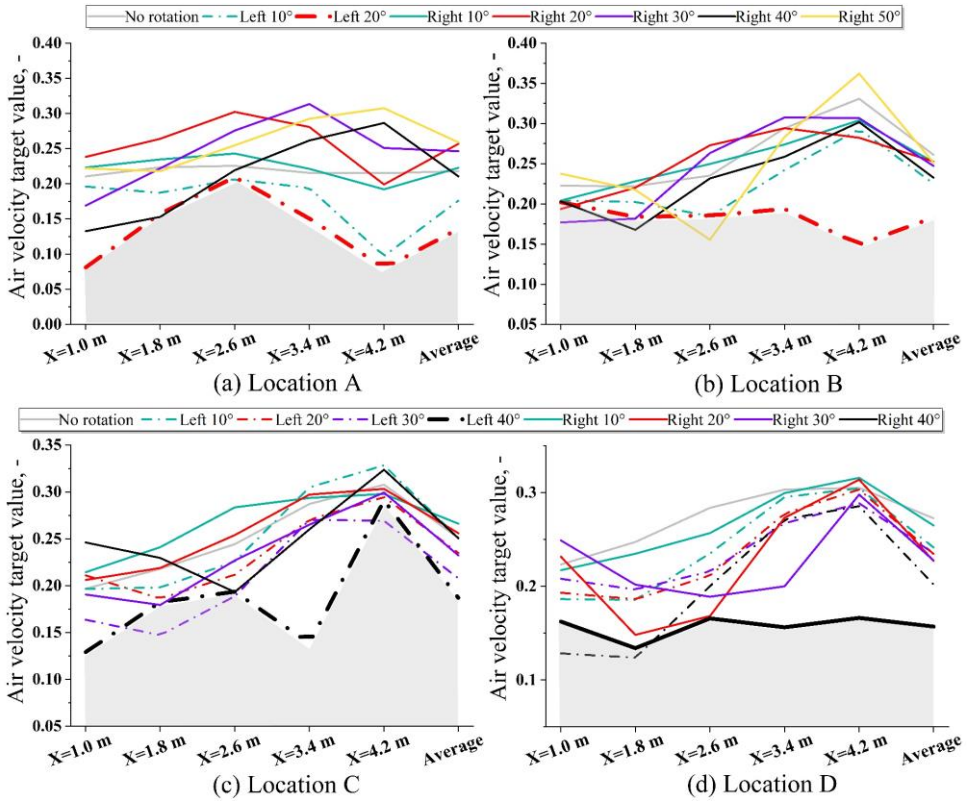

Figure 11: Recommended rotation angles for different locations in the Z-direction (long side of the room) when the air supply velocity is 2 m/s.

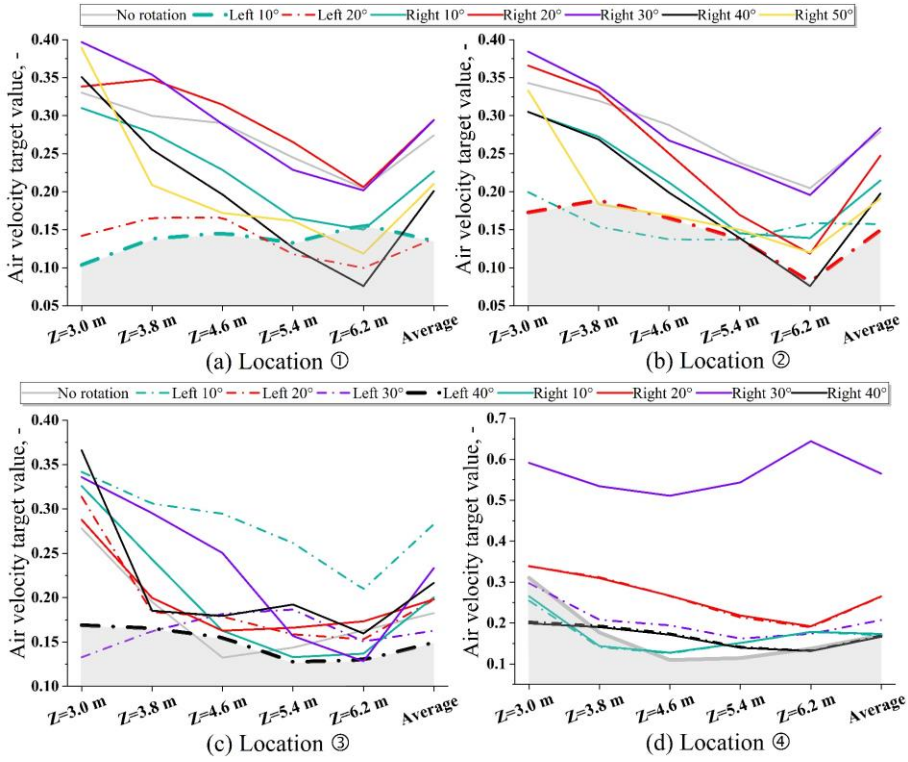

Figure 12: Recommended rotation angles for different positions in the X-direction (short side of the room) when the air supply velocity is 3 m/s.

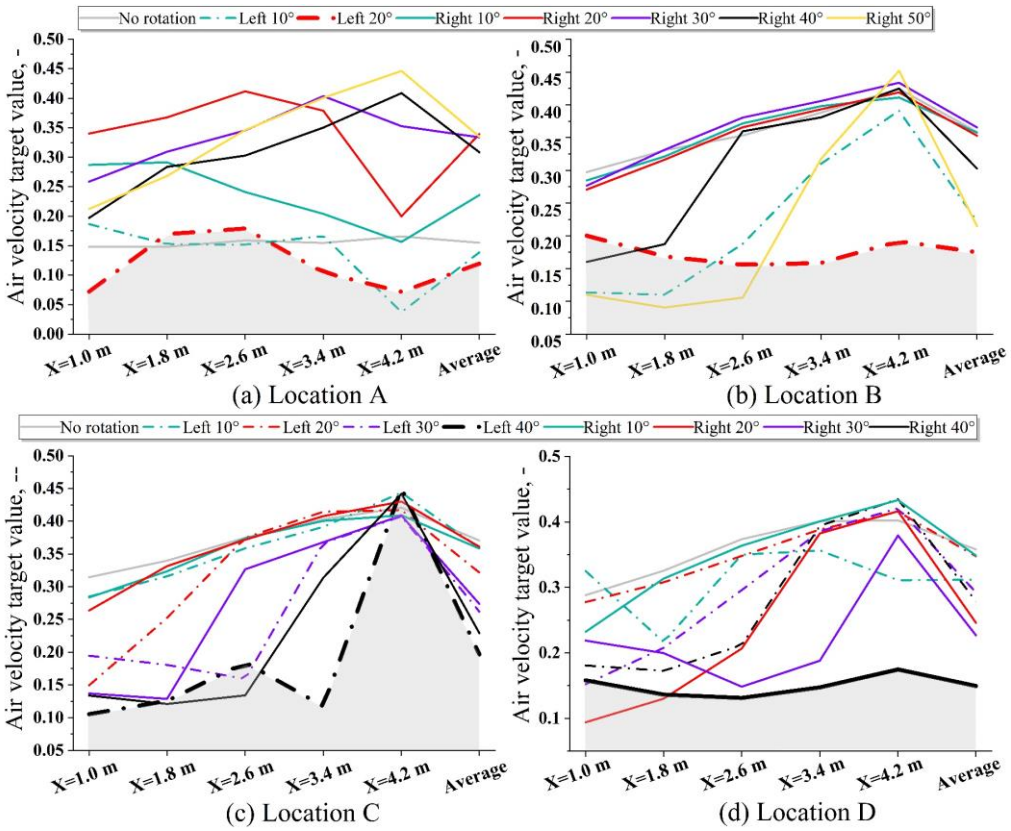

Figure 13: Recommended rotation angles at different positions in the Z-direction (long side of the room) when the air supply velocity is 3 m/s.

From the comparison in Fig. **13**, it can be seen that at position A, when the air conditioner is rotated left at 20°, the two plane velocity target value and the average value of five planes are the smallest; at position B, when the air conditioner is rotated left at 20°, the overall velocity target value are below 0.2, and the distribution is more uniform; at position C, when the air conditioner is rotated left at 40°, three planes velocity target value and the average value of five planes are the smallest; at position D, when the air conditioner is rotated right at position D when the air conditioner is turned to the right at 40°, the four plane velocity target value and the average value of the five planes are the smallest. The above angle can be regarded as the recommended rotation angle of the air conditioner.

From Fig. **12** and Fig. **13**, it can be seen that the fluctuation range of the velocity target value of the five planes is larger than that of 2 m/s, with most of the values concentrated in the range of 0.05-0.45. The difference between the values is large, making it relatively easy to determine the "recommended angle."

4.3. Indoor Flow Analysis

The results of the above simulation are summarized in Table **2**. The analysis found that the recommended rotation angles differed at the same air conditioning outlet velocity, corresponding to different air conditioning locations; the recommended rotation angles were also different at the same locations under different air supply velocities.

Table 2: Recommended rotation angle in different locations with different velocity of air conditioning.

Air Velocity	Location A	Location B	Location C	Location D	Location①	Location②	Location③	Location④
1m/s	turn right 50°	non rotation	turn left 30°	turn left 40°	turn left 10°	turn left 20°	turn left 30°	turn left 20°
2m/s	turn left 20°	turn left 20°	turn left 40°	turn right 40°	turn right 50°	turn left 20°	turn left 20°	turn right 30°
3m/s	turn left 20°	turn left 20°	turn left 40°	turn right 40°	turn left 10°	turn left 20°	turn left 40°	non rotation

For example, at position A, the best angle at air velocity 1 m/s is 50° to the right, and the best angle at air velocity 2 m/s and 3 m/s is 20° to the left, with the same recommended angle at two air velocity. The recommended rotation angles are different for each air velocity at position ③, and this section analyzes the reasons for this phenomenon through the indoor velocity flow diagram.

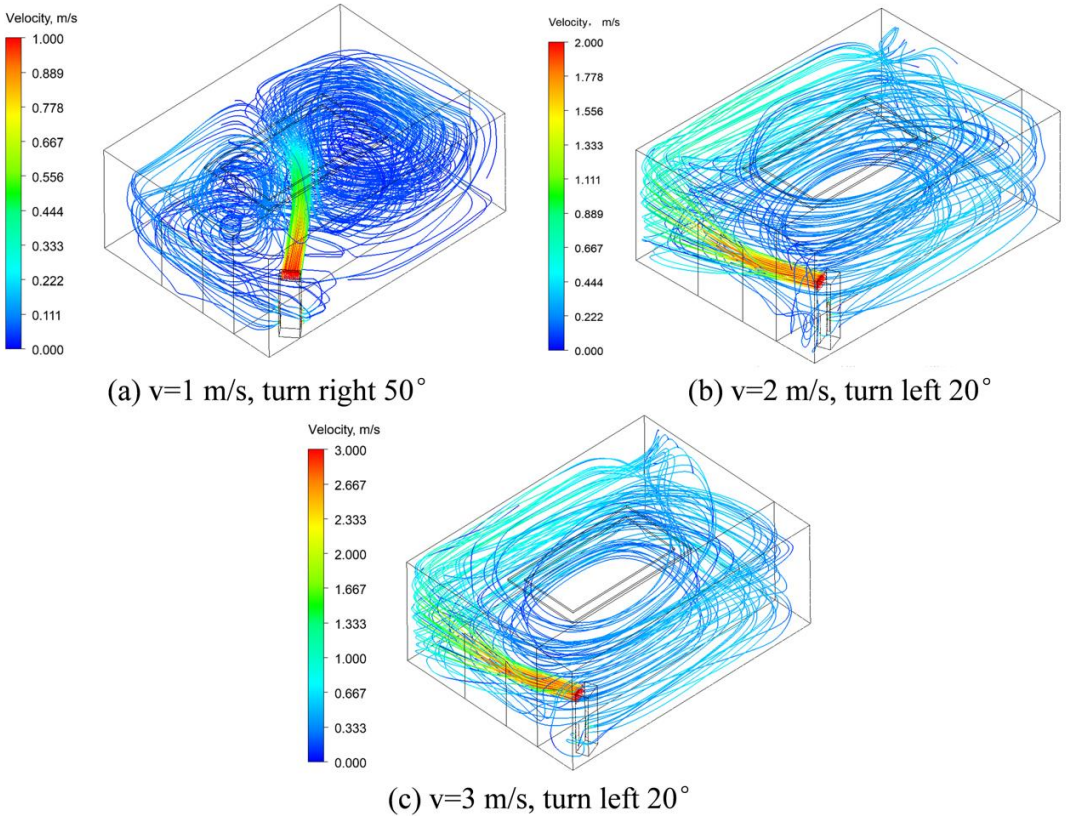

Figure 14: Indoor flow diagram of the best rotation angle of the air conditioner at location A for three air velocities.

At location A, it can be seen from Fig. **14(a)** that at an outlet air velocity of 1 m/s, when the air conditioner is turned 50° to the right, although the outlet air is sent directly to the personnel work area, the velocity has dropped to 0.5 m/s at the height of 2 m by the time it reaches the work area, and the velocity is even lower at the height of 1.8 m. According to the draft rate model developed by Fanger *et al*. [26], local air velocities higher than 0.3 m/s are regarded as high velocities that affect the draft, so it basically does not cause a draft sensation at this time.

From the analysis in Fig. **14(b and c)**, when the air velocity is 2 m/s and 3 m/s, if the previous angle is still maintained so that the air conditioning air is blown directly to the personnel work area, it will cause high air velocity in the work area. So the recommended angle is turn left at 20°, so that the high speed airflow is not blow directly to the work area, but hits the wall and flows around the wall. Here the velocity in occupied zone is basically near 0.3 m/s, the calculated velocity target value in occupied zone is lower, reduced the draft sensation to a certain extent.

At position ③, the recommended air conditioning angles at different air velocities are deflected, and no angle blows directly into the work area. As can be seen from Fig. **15**, when the air velocity is 1 m/s, part of the outgoing airflow is sent directly to the personnel work area, and part of the airflow returns to the personnel work area after impacting with the wall, and the air velocity is all below 0.4 m/s, which can reduce draft sensation in the work area. When the air velocity is 2 m/s, the airflow is sent along the side wall and the opposite wall for attachment flow, forming a circular flow in the whole room to avoid the high air velocity in the work area and effectively reduce the draft sensation. When the air velocity is 3 m/s, the deflection angle of the air conditioner is larger, the airflow first flows along the side wall, and then part of the airflow flows along the opposite wall and form a circular flow in the space, the other part of the airflow forms a vortex after hitting the opposite wall and returns to the personnel working area after the velocity is attenuated, effectively reducing the air velocity in the working area.

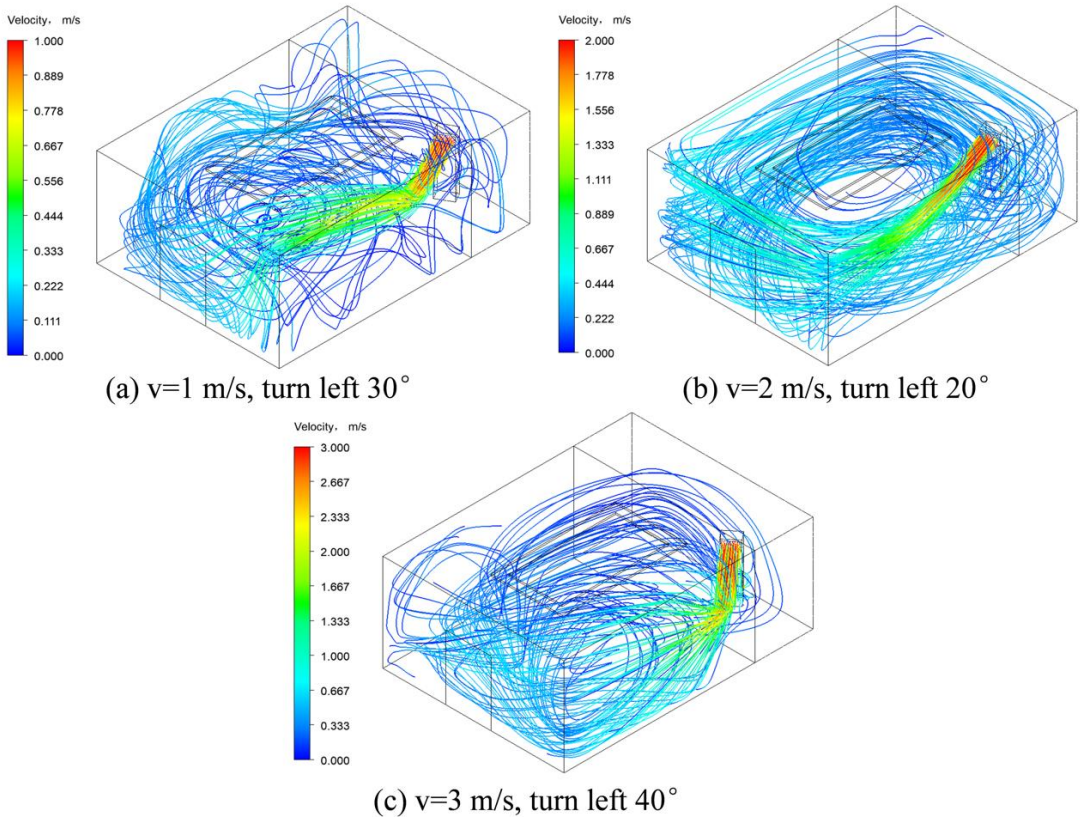

Figure 15: Indoor flow diagram of the best rotation angle of the air conditioner at location ③ for three air velocities.

5. Conclusion

Based on the valuable conclusions and shortcomings of previous studies on floor-standing room air conditioners, this paper studies the recommended placement and air distribution of floor-standing room air conditioners. The main conclusions are as follows:

Based on the air velocity target value form proposed by the previous research group, the air velocity target value equation that only needs to evaluate the air supply effect in the working area is proposed. Taking the velocity target value as the evaluation index, a total of 204 working conditions are numerically simulated. The recommended rotation angles of the air conditioner in eight different locations are obtained under the conditions of no rotation, left rotation at a certain angle, right rotation at a certain angle, and so on under the three air outlet velocities of 1 m/s, 2 m/s, and 3 m/s.

It is found that the velocity target value of different plane working areas of the room under the optimal rotation angle is basically below 0.25. The recommended rotation angle is different at different air conditioning locations in the room under the same air velocity. The recommended rotation angle is different under different air supply velocities when the air conditioner is placed in the same location. Taking two placement positions as examples, combined with the indoor velocity streamline diagram, the causes of this phenomenon are analyzed.

The full-scale experiment found that the numerical simulation results are consistent with the experimental results, which verifies the reliability of the data. Then the possible reasons for the slight error between the experimental results and the simulation value are analyzed.

The limitation of this study is that only the velocity target value is taken as the index, and only the velocity field distribution is considered; the temperature distribution is not considered. The temperature field distribution can be studied later.

Acknowledgment

This work was supported by the Opening Funds of the State Key Laboratory of Building Safety and Built Environment & National Engineering Research Center of Building Technology (Grant No. BSBE2019-08). We mention that the authors contributed equally.

References

[1] 2020 China Building Energy Consumption Research. 2020.

[2] Hu S, Yan D, Qian M. Using bottom-up model to analyze cooling energy consumption in China's urban residential building. Energy Build 2019; 202: 109352. https://doi.org/10.1016/J.ENBUILD.2019.109352.

[3] He Y, Li N, Peng J, Zhang W, Li Y. Field study on adaptive comfort in air conditioned dormitories of university with hot-humid climate in summer. Energy Build 2016; 119: 1–12. https://doi.org/10.1016/J.ENBUILD.2016.03.020.

[4] Buonocore C, de Vecchi R, Scalco V, Lamberts R. Influence of recent and long-term exposure to air-conditioned environments on thermal perception in naturally-ventilated classrooms. Build Environ 2019; 156: 233–42. https://doi.org/10.1016/J.BUILDENV.2019.04.009.

[5] Chao CYH, Wan MP. Airflow and air temperature distribution in the occupied region of an underfloor ventilation system. Build Environ 2004; 39: 749–62. https://doi.org/10.1016/J.BUILDENV.2004.01.010.

[6] National Bureau of Statistics of China. China Statistical Yearbook 2021. Beijing: China Statistics Press; 2021.

[7] Wang Y, Kuckelkorn J, Zhao FY, Liu D, Kirschbaum A, Zhang JL. Evaluation on classroom thermal comfort and energy performance of passive school building by optimizing HVAC control systems. Build Environ 2015; 89: 86–106. https://doi.org/10.1016/J.BUILDENV.2015.02.023.

[8] Huang SY, Zhao F, Li G. Numerical simulation study on the thermal environment of an air-conditioned in summer based on Airpak. Journal of Hunan University of Science and Technology 2011; 26: 11–7.

[9] Liu W. Study on Objective Evaluation Index of Human Thermal Comfort. Doctoral dissertation, PhD Thesis. Shanghai Jiao Tong University, 2007.

[10] Liu W, Lian Z, Yao Y. Optimization on indoor air diffusion of floor-standing type room air-conditioners. Energy Build 2008; 40: 59–70. https://doi.org/10.1016/J.ENBUILD.2007.01.010.

[11] Yin G. The indoor thermal comfort research of the air conditioning mode in large space. University of South China, 2009.

[12] Zhang Z, Gao R, Liu Y, Liu M, Wang Y, Zhu W, *et al*. Smart air supply terminal for floor-standing room air conditioners based on the identification of human positions. Build Environ 2021; 202: 108041. https://doi.org/10.1016/J.BUILDENV.2021.108041.

[13] Li Y. Study on indoor airflow organization and thermal comfort of air conditioning system in the office building. North China University of Technology, 2017.

[14] Gao CF, Lee WL. Optimized design of floor-based air-conditioners for residential use. Build Environ 2009; 44: 2080–8. https://doi.org/10.1016/J.BUILDENV.2009.02.011.

[15] Xin S, Xu H, Li S, Wang W, Guo J, Yang W. Efficiency evaluation of a floor standing air conditioner with different installation positions and air supply parameters applied to a large laboratory. Journal of Building Engineering 2020; 32: 101701. https://doi.org/10.1016/J.JOBE.2020.101701.

[16] Ma R. Displacement ventilation effectiveness and evaluation of the micro thermal environment. Journal of HVAC 1997; 27: 1–6.

[17] Li X, Zhao B. Numerical simulation of indoor airflow. Mechanical Industry Press; 2009.

[18] Fanger PO. Thermal comfort. Analysis and applications in environmental engineering. Copenhagen: Danish Technical Press; 1970.

[19] Wang X, Liu T, Lee WL. Using revised ADPIs to identify an optimum positioning for installation of reversible room air-conditioners in bedroom for maximum thermal comfort. Build Environ 2021; 188: 107333. https://doi.org/10.1016/J.BUILDENV.2020.107333.

[20] Gao R, Wang C, Li A, Yu S, Deng B. A novel targeted personalized ventilation system based on the shooting concept. Build Environ 2018; 135: 269–79. https://doi.org/10.1016/J.BUILDENV.2018.03.016.

[21] Gao R, Zhang H, Li A, Wen S, Du W, Deng B. A new evaluation indicator of air distribution in buildings. Sustain Cities Soc 2020; 53: 101836. https://doi.org/10.1016/J.SCS.2019.101836.

[22] Chen Q. Comparison of different k-ε models for indoor airflow computations. Numerical Heat Transfer, Part B: Fundamentals 1995; 28: 353–69. https://doi.org/10.1080/10407799508928838.

[23] Ye X, Zhu H, Kang Y, Zhong K. Heating energy consumption of impinging jet ventilation and mixing ventilation in large-height spaces: A comparison study. Energy Build 2016; 130: 697–708. https://doi.org/10.1016/J.ENBUILD.2016.08.055.

[24] Rouaud O, Havet M. Computation of the airflow in a pilot scale clean room using K-ε turbulence models. International Journal of Refrigeration 2002; 25: 351–61. https://doi.org/10.1016/S0140-7007(01)00014-7.

[25] ASHRAE. ANSI/ASHRAE Standard 55-2017: Thermal Environmental Conditions for Human Occupancy. ASHRAE Inc 2017; 2017.

[26] Fanger PO, Melikov AK, Hanzawa H, Ring J. Air turbulence and sensation of draught. Energy Build 1988; 12: 21–39. https://doi.org/10.1016/0378-7788(88)90053-9.